

Analysis of Effective Signal Design for Active Sensing of Undersea Objects/Bottoms in Tropical Shallow Waters

Arnab Das, Venugopalan Pallayil
Acoustic Research Lab,
Tropical Marine Science Institute,
National University of Singapore, Singapore

Abstract—Precise understanding of the sea bottom characteristics and accurate identification of objects on the seabed are critical in many underwater applications. The severe multi-path along with the time varying and random reflections from the surface and the bottom of shallow waters, present an interesting and complex signal processing problem. A thin line hydrophone array, deployed from small Autonomous Underwater Vehicles (AUV) provides significant operational advantage in terms of accessibility in shallow coastal areas and does open up substantial application possibilities. The shallow tropical waters in general present high ambient noise levels due to high density snapping shrimp beds and shipping. This often requires that for getting a reasonably good Signal to Noise Ratio (SNR) the acoustic transmissions have to be powerful to combat the noise level. However, this is not a good option for many battery powered platforms like an AUV as it heavily limits their operational endurance. An alternative is to design specific sonar signals which have high correlation properties and can provide good detection performance under severe noise conditions. Although the sonar waveform design is not new, such application specific signal processing attempt is not reported in the literature. The work will present a two-stage, Non-Linear Frequency Modulated (NLFM) signal design for active undersea sensing using a Digital Thin Line Array (DTLA). The signal design has been undertaken for the frequency band 3-10 kHz, with variations in center frequency and bandwidths. The different chirp rates in a two-stage LFM signal and non-LFM were evaluated for their effectiveness in suppressing the side lobes. The bottom reflected signal has been correlated with the direct path signal, to allow minimal difference between the received signal and the receive filter characteristics, due to the underwater channel. The well-known shallow water propagation loss model proposed by Rogers (1974) was used to simulate the underwater channel conditions in shallow water conditions. The performance metric was based on the ability to minimize the integrated side lobe level metric (ISL) of the normalized correlation function. Bottom types comprising sand and silt have been used in the simulated channel model to compare the performance.

Keywords—Bottom characterization, tropical shallow waters, active sensing, sonar waveform design, side lobe suppression, Thin Line Array.

I. INTRODUCTION

Bottom characterization (rock, sand, mud, silt, etc.) is critical for precise underwater channel modeling and subsequent mitigation of propagation related modification of the desired signal [1]. Sea bottom characterization could also be useful for fish habitat study, geological studies, marine explorations, undersea mining and many other applications [2-4]. The identification of underwater object is important, especially for defense application, to accurately recognize undersea/buried mines [5] and could also be critical for multiple non-military applications like maintenance/repair of undersea structures, marine sciences, etc. [6-9].

The active acoustic sensing is an obvious choice for such applications, where a probing waveform is transmitted and the echo returned by the target is processed to extract useful information regarding characteristics of the target. The target here could be the sea bottom itself or objects on the seabed and buried. Thus, a good design of the probing waveform could significantly enhance the system performance that may include target parameter estimation, signal-to-noise ratio, spectral containment, interference suppression etc. [10].

The recent increase in underwater sensing requirements both for both military and non-military applications, in the shallow waters has introduced newer challenges in signal design [11]. The development of miniaturized sensing hardware like the Digital Thin Line Arrays (DTLA), and its integration with small platforms like the AUV, has opened up enhanced accessibility for undersea sensing in extremely shallow waters [12]. However, the limitations of tropical shallow waters, like off Singapore coast, will require special signal design efforts to overcome the poor SNR conditions and the severe UW channel distortions. The smaller platforms like AUVs, which runs on battery power, put additional power restrictions and thus, higher transmission power levels to overcome the poor SNR is not a good option.

The matched filters have been the well-known receiver models for maximizing the SNR in the presence of stochastic additive noise [13]. Another technique is the matched field processing that has been successfully used in

the UW sensing, however, requires significant understanding of the UW channel properties [14]. Other receiver filter techniques reported in literature are the instrumental variable method [15], the Capon estimator [16], the amplitude and phase estimator algorithm [17] and the iterative adaptive approach [18].

The linear frequency modulated (LFM) signal designs have been popular as a pulse compression tool for radar and sonar applications, and have enabled long range detection and good resolution simultaneously [19]. However, the LFM signals have poor side lobe suppression abilities due to mismatch losses and would require pulse shaping (making them non-linear) to enhance main lobe to side lobe separation [20]. The two-stage LFM (thus, Non-Linear FM) is presented as a simple but yet provides SNR enhancement over the LFM signal [21].

The conventional tool for sonar signal evaluation is the correlation function represented by the function [10]:

$$r[k] = \sum_{n=0}^{N-1} s[n] s^*[n+k], -(N-1) < k < (N-1), \quad (1)$$

Where, $s[n]$ is the complex envelope of the probing signal, k is the round-trip time delay, and n indicates the time. $s^*[n+k]$ is the echo returned at the receiver, $r[k]$ is the correlation function at lag k . The typical performance measure for a correlation function is the Integrated Sidelobe Level (ISL) metric defined as [10]:

$$ISL = \sum_{k=-N+1}^{N-1} |r[k]|^2 = 2 \sum_{k=1}^{N-1} |r[k]|^2 \quad (2)$$

The performance optimization will call for minimization of the ISL metric. Conversely, we also seek to maximize the merit factor (MF), defined as [10]:

$$MF = \frac{|r(0)|^2}{\sum_{k=-N+1}^{N-1} |r[k]|^2} = \frac{N^2}{ISL} \quad (3)$$

In this work we have attempted to evaluate the SNR enhancement abilities of various two stage LFM signal designs in tropical waters off Singapore. The matched filter receiver advantage has been derived using the correlation model by correlating the direct path signal with the bottom return signal. The signal modification due to the volume interactions in the medium has been obviated using the direct path signal as a reference signal [12]. The underwater channel has its own influence on the bottom echo and even the direct path signal, thus the bandwidth, slope of LFM, pulse width, etc., need to be optimized to derive the suitable transmitted signal [22].

The underwater channel model has been simulated based on the well-known Rogers model [23], known for shallow channels. The probing signal has been passed through the channel model to evaluate the signal deterioration due to the medium. The experimental area has been taken as 20 m deep with the transmitter and receiver placed at 5 m depth and 50 m apart as shown in Fig. 1

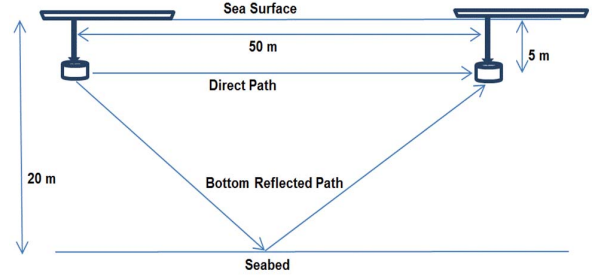


Fig. 1. Schematic Representation of the Experiment

II. SIGNAL DESIGN

In any radar or sonar system deployed for active sensing, two aspects become critical for system performance. The first is the receiver design and second, the transmitted waveform characteristics. A judicious signal design of the probing signal can considerably enhance the target detection and estimation performance and plays a crucial role in the receiver implementation and efficiency of the system. The performance of the signal design can be evaluated using one of the multiple measures of quality depending on the application. The signals with good correlation properties have been commonly used in active sensing. This essentially implies that we have a matched filter receiver design to ensure higher concentration of spectral energy in the main lobe. The optimum signal design has to make sure the impulse like correlation metrics with minimal side lobe energy [10].

The Linear Frequency Modulated (LFM) signal has better range performance and SNR over the conventional pulsed Continuous Wave (CW), given that the system has low-noise electronics, and wide, equalized amplitude bandwidth that is supported by the transducer and the receiver. LFM has time-bandwidth product more (more often much more) than one, so is able to simultaneously achieve high range resolution and longer range [20]. The bandwidth, frequency modulation slope and pulse width of the probing signal can be varied to extract target parameters from the return.

The LFM signal is constructed by rectangle transmitting pulse whose width is τ and carrier frequency f_0 , that increases linearly between f_1 to f_2 . The bandwidth B is defined as $B = \Delta f = f_2 - f_1$, centered around the frequency f_0 and the frequency modulation slope is defined as $k = B/\tau = \Delta f/\tau$. The transmitting pulse, $s(t)$ is thus represented as [10]:

$$s(t) = e^{-j2\pi(f_0 t + (B/2\tau)t^2)}, \quad -\tau/2 < t < \tau/2 \quad (4)$$

The spectrum of the transmitted signal is represented as

$$S(f) = \int_{-\tau/2}^{\tau/2} e^{j\{(f_0 - f)t + (B/2\tau)t^2\}} dt \quad (5)$$

The pulsed signal $x(t)$, with the shaping pulse $p(t)$ can be represented as

$$x(t) = s(t)p(t), \quad -\tau/2 < t < \tau/2 \quad (6)$$

The ideal rectangular shaping, pulse is written as

$$p(t) = \left(1/\sqrt{\tau}\right) \text{rect}(t), \quad \text{rect}(t) = \begin{cases} 1, & -\tau/2 < t < \tau/2 \\ 0, & \text{otherwise} \end{cases} \quad (7)$$

The shaping pulse can be varied based on the application. Typically, the rectangular pulse or no pulse shaping over an LFM signal provides only -13.2 dB separation between the main lobe and the side lobe [21]. Weighting functions or window functions, like the Hamming window, have been reported to enhance the side lobe suppression, with the cost of broadening of the main lobe, thereby proportionately compromising the range resolution [24]. Further, the weighting also causes mismatch between the signal spectrum and the filter transfer function resulting in “mismatch losses”. The mismatch losses are of the order of 1.5 dB and vary with the degree of weighting [20].

The Hamming window with the window function given as

$$P(f) = 0.54 + 0.46\cos(\pi f), \quad |f| \leq 1 \quad (8)$$

The Raised cosine window with the window function given as

$$P(f) = \cos^4(0.7\pi f), \quad |f| \leq 1 \quad (9)$$

The Truncated Gaussian window with the window function given as

$$P(f) = \exp\left(-K\left(f/2\right)^2\right), \quad |f| \leq 1 \quad (10)$$

The constant K is selected to be 13.8155, giving an attenuation of 30 dB at the edge of the window [20].

We see the impact of the window functions in fig. 2 above. The left of the figure represents the ideal window impact and more or less matches with the theoretical auto-correlation advantage. The raised cosine window gives upto 44 dB gain, compared to the 17 dB (13.2 dB theoretically) for rectangular window or no window. We discuss the right side of the fig. 2, subsequently in the channel impact section. The Gaussian window function has been used for the non-linear FM transmit signal design as no significant advantage has been observed post the channel.

The mismatch losses can be minimized by employing a multi-stage LFM signal, where the slope of the frequency increase is modified in steps, instead of a single sweep [20]. The two-stage Non Linear Frequency Modulation (NLFM) is a simple to implement technique for improving the correlation properties of the signal at the receiver. The frequency of each stage is linearly swept through the given time frame as given below and also pictorially represented in fig. 3:

$$f(t) = \begin{cases} \frac{B_1}{T_1}t, & 0 \leq t \leq T_1 \\ B_1 + \frac{B_2}{T_2}(t - T_1), & T_1 \leq t \leq T_2 \end{cases} \quad (11)$$

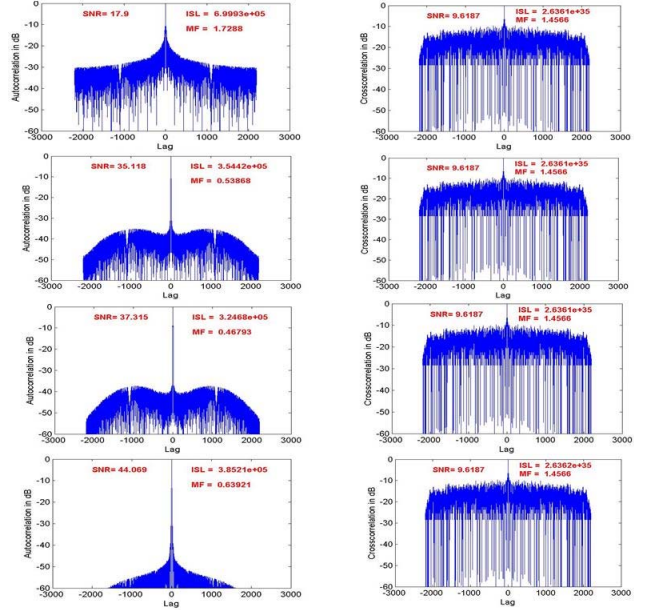


Fig. 2. Comparison of signal before and after the channel.
Left (a): Auto-correlation of the signal at source
Right (b): Cross-correlation of the direct path and the bottom reflected path.
From Top: I-Rectangular, II-Gaussian, III-Hamming and IV-Raised Cosine of the Experiment

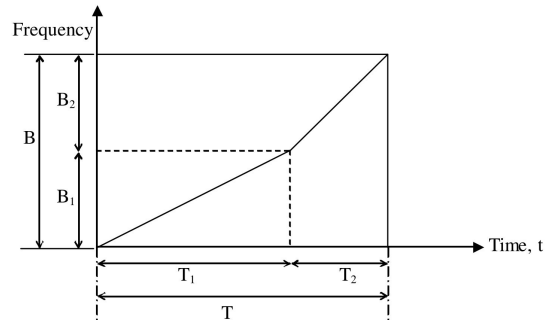


Fig. 3 Modulation signal of simple two stages NLFM waveform [21].

Varying the values of B1, B2, T1 and T2, we simulate the probing signals to evaluate its performance in the underwater channel for its correlation performance at the receiver. The time and bandwidth distribution has been so chosen to get a good representation of the signal variation both in the time and frequency axis. Table-2, presents the detailed signal design used in this work along with the results obtained.

III. CHANNEL DISTORTION

The simulation of the probing signal and its received counterpart is not complete without the consideration of the channel impact. The channel model thus, becomes critical to our simulation efforts. There are multiple channel models proposed by numerous researchers to suit specific channel conditions and application requirement [25]. We use the

Rogers model [23] for its simplicity in explaining the propagation loss for a shallow water channel. The signal model used in this work is a simplistic mathematical model given below:

$$y(t) = x(t) * h(t) + w(t) \quad (12)$$

Where, $y(t)$, is the signal at the receiver,

$x(t)$, is the signal at source,

$h(t)$, is the channel impulse response, and

$w(t)$, is the ambient noise at the receiver.

The Rogers model presented a way to predict acoustic attenuation in shallow water subject to mode stripping and cylindrical propagation. Two distinctions are made while formulating the attenuation formula. The following attenuation formula is valid when the effective angle of the last mode stripped $\theta_g \geq \theta_L = \max\{\theta_{g \max}, \theta_c\}$, where $\theta_{g \max}$ is the maximum grazing angle for a Refracted-Bottom-Reflected (RBR) mode and θ_c is the cutoff angle of the lowest mode [25]:

$$A(d, f) = 15 \log_{10} d + 5 \log_{10}(h\beta) + \frac{\beta d \theta_L^2}{4h} - 7.18 + \alpha(f)d \quad (13)$$

When $\theta_g < \theta_L$, we use the formula

TABLE I. BOTTOM LOSS COEFFICIENT VALUES B OF TYPICAL BOTTOM TYPES AND THE RESULTS

S.No.	Sediment Type	β	ISL	MF	SNR(dB)
1.	Sand	Coarse	2.063	1.5205 e ³⁵	1.4566
		Fine	3.093	2.6361 e ³⁵	1.4566
		Very Fine	3.587	3.2794 e ³⁵	1.4566
2.	Silty sand	4.3663	4.4369 e ³⁵	1.4566	9.6187
3.	Sandy Silt	21.262	7.2461 e ³⁶	1.4566	9.6187
4.	Silt	5.6157	6.6569 e ³⁵	1.4566	9.6187
5.	Sand-silt-clay	11.9648	2.4874 e ³⁶	1.4566	9.6187
6.	Clayey silt	34.8171	1.8637 e ³⁷	1.4566	9.6187
7.	Silty clay	85.3214	1.0758 e ³⁸	1.4566	9.6187

IV. RECEIVER DESIGN

The probing signal $x(t)$ is emitted in almost all the directions, but we are interested in that part of the signal that is received at the receiver. Three signals are of interest to us at the receiver. The first is the direct path signal that travels directly from the transmitter to the receiver suffering spreading loss and the volume attenuation loss. The second is the surface reflected path that comprises of three loss factors, namely the spreading loss, the volume attenuation loss and the surface reflected loss (normally negligible). The third is the bottom reflected path that again consists of three loss factors, namely the spreading loss, the volume attenuation and the bottom reflection loss. In the real experimental recording the understanding of the geometry of the signal path may be critical in identifying the different returns within the received signal.

The three signals at the receiver can be separated based on the travel time as the direct path will have the least path delay and the Refracted Bottom Reflected (RBR) path will have the maximum path delay. The surface reflected path is ignored as the deployment of the transmitter from the AUV or any

$$A(d, f) = 10 \log_{10} d + 10 \log_{10} \left(\frac{h}{2\theta_L} \right) + \frac{\beta d \theta_L^2}{4h} + \alpha(f)d \quad (14)$$

Where, d is the transmitter-receiver range (in m), h is the uniform height of the water column (in m), β is the bottom loss coefficient (in dB/rad) determined from the Rayleigh reflection coefficient, and $\alpha(f)$ is Thorp's absorption loss factor. This is an approximate model that estimates the large number of underwater conditions into just three parameters namely h , β and $\alpha(f)$, that represent the spreading losses, bottom losses and the volume attenuation losses. The model is a range independent model with an assumption of flat bottom using average depth value. We have undertaken simulations for varying β values as shown in table-1 and fig. 4. The β values have been computed using formulae given in Rogers work [23]. The channel and bottom type analysis has been undertaken using a Gaussian window for LFM signal with pulse length of 100 ms and bandwidth of 3-10 kHz. The sampling frequency used is 22 kHz for all the signal simulation in this work. The absorption loss factor $\alpha(f)$, as a function of frequency stabilizes at high frequency beyond 2 kHz and maintains a value approximately 0.8. Table-1 is discussed subsequently in section V.

other platform used will block the signal towards the surface and thus will not be received at the receiver and also this being a simulated study. We correlate the direct path and the RBR path signal to derive the correlation metrics at the matched filter receiver. The reference signal of the matched filter is the direct path signal and that provide the advantage to encompassing the underwater channel fluctuations and minimizing the mismatch with the RBR path signal.

The simulation of the direct path signal has been undertaken using the appropriate components from equations (13) or (14) and similarly the RBR path signal has been generated using the equations (13) or (14) depending upon the effective angle of the last mode stripped. MATLAB code has been used to undertake all the simulations. Fig. 2, presents the signal at source and the receiver for the window types described in table-2 for simple LFM.

TABLE II. COMPARISON OF WINDOW FUNCTION

S.No.	Signal Type	Window Function	ISL	MF	SNR (dB)
01	Singletone 5 kHz	Rectangular	1.8431 e ³⁸	0.002083	0.0584
	Singletone	Rectangular	1.8479 e ³⁸	0.002078	0.0024

	8 kHz				
02	Linear Frequency Modulated (LFM) Signal.	Rectangular	$2.6361 e^{35}$	1.4566	9.6187
		Hamming	$2.6361 e^{35}$	1.4566	9.6187
		Raised Cosine	$2.6362 e^{35}$	1.4566	9.6187
		Gaussian	$2.6361 e^{35}$	1.4566	9.6187

Fig. 2, brings out the substantial deterioration in the signal received through the channel. The theoretical gain of a window function in suppressing the side lobe is substantially lost as the signal propagates through the underwater channel. The 44 dB gain of a raised cosine window is reduced to 9.6187 dB after the channel and similarly even the other window also show deterioration. Table-2, also brings out another aspect of the underwater channel, wherein we find that in severe channel condition, signal like a pure tone may be degraded to a very significant degree, making it unusable for any meaningful analysis. Thus, special kinds of probing signal design becomes mandatory in many underwater sensing applications.

V. RESULTS & DISCUSSIONS

The transmit signal has been passed through the underwater channel with varying bottom types and the Rogers model has been used to model the environment. The first set of simulations was carried out for varying bottom types (see Table-1) with the channel geometry as described in fig. 4.

The evaluation of the impact of bottom type has been undertaken using the three parameters, namely, Integrated Side lobe Level (ISL), Merit Factor (MF) and the SNR representing the main lobe to side lobe separation in dBs as enumerated in

section I. The bottom loss coefficient \square value is observed to be increasing as we progressively move from sand to silt. Higher value of bottom loss coefficient means poorer reflection.

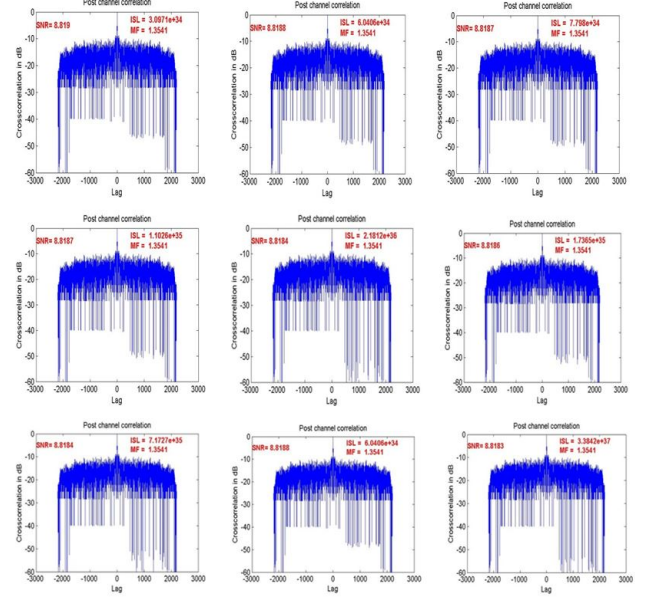


Fig. 4. Evaluation of the varying bottom types.
Top row: Sandy bottom from left to right - Coarse, Fine and very fine.
Middle row: Left to right - Silty sand, sandy silt and silt. Bottom row: Left to right - Sand-silt-clay, clayey silt and silty clay.

TABLE III. COMPARISON OF WINDOW FUNCTION

S.No.	Signal Type	Bandwidth	Time	ISL	MF	SNR(dB)
01	Two stage Non-LFM.	B1=3 -5 kHz. B2=5 - 10 kHz	T1=20 msec, T=100 msec.	$7.191 e^{35}$	0.5339	11.734
		B1=3 -6 kHz. B2=6 - 10 kHz	T1=20 msec, T=100 msec.	$3.0786 e^{35}$	1.1405	7.6274
		B1=3 -7 kHz. B2=7 - 10 kHz	T1=20 msec, T=100 msec.	$4.5602 e^{35}$	0.8419	10.086
		B1=3 -8 kHz. B2=8 - 10 kHz	T1=20 msec, T=100 msec.	$7.191 e^{35}$	0.5339	11.734
02	Two stage Non-LFM.	B1=3 -5 kHz. B2=5 - 10 kHz	T1=40 msec, T=100 msec.	$6.8736 e^{34}$	1.278	9.1964
		B1=3 -7 kHz. B2=7 - 10 kHz	T1=40 msec, T=100 msec.	$3.157 e^{35}$	1.2159	8.3174
		B1=3 -9 kHz. B2=9 - 10 kHz	T1=40 msec, T=100 msec.	$9.324 e^{35}$	0.4118	7.9349
03	Two stage Non-LFM.	B1=3 -5 kHz. B2=5 - 10 kHz	T1=70 msec, T=100 msec.	$6.8736 e^{34}$	1.278	9.1964
		B1=3 -7 kHz. B2=7 - 10 kHz	T1=70 msec, T=100 msec.	$3.1578 e^{35}$	1.2159	8.3174
		B1=3 -9 kHz. B2=9 - 10 kHz	T1=70 msec, T=100 msec.	$9.324 e^{35}$	0.4118	7.9349

(a) the mainlobe to sidelobe separation really does not get significantly impacted by the bottom type as the channel deterioration is significant. The MF and SNR values remain same till four decimal places.

(b) The difference is though observed in the ISL values and a direct relation is seen with respect to the bottom loss coefficient \square . Thus, ISL could be a better measure to identify the bottom type.

By analyzing the results presented in table-2 and based on the geometry shown in fig.4, we draw following conclusions:

(c) Choice of window function does not have a significant impact on the correlation function post channel.

The different signal types were also evaluated in the similar manner using ISL, MF and SNR. Table-3, presents the results of the varying signal types using the same performance criterion

The two-stage NLFM signal design does present some SNR advantage over the simple LFM. There is a pattern observed when we analyze the results presented in table-3. The $B1=3-5$ kHz and $B2=5-10$ kHz for $T1=20$ ms and $T2=100$ ms does give high performance and another symmetric signal $B1=3-8$ kHz and $B2=8-10$ kHz for $T1=20$ ms and $T2=100$ ms gives equally good results of 11.734 dB SNR and 7.191e35 ISL. Other combinations give intermediate results and some even going below a simple LFM. The combination $B1=3-5$ kHz and $B2=5-10$ kHz for $T1=40$ ms and $T2=100$ ms, becomes similar to the simple LFM so we get more or less similar performance of 9.1964 dB SNR and 6.8736e34 ISL

VI. CONCLUSION AND FUTURE SCOPE

The underwater sensing in tropical shallow waters present a significant challenge to any sonar designer. The multiple interaction with the surface and the bottom make the system performance highly sensitive to the bottom and surface characteristics. Severe degradation is observed in the conventional transmit signal pulse and with high noise levels maximum SNR gain is desired during the signal processing at the receiver. In this work we observe that the severe channel deterioration makes the conventional signal design redundant for any meaningful analysis on the received signal. Thus, probing signal design does become critical to obtain reasonable SNR at the receiver to further analyze the received signal for bottom characterization or object identification applications. The channel deterioration in the tropical littoral waters make the choice of window function redundant, particularly for a matched filter receiver model. The Integrated Sidelobe Level (ISL) measure does provide reasonable difference among the various post channel cross-correlation functions to draw conclusion.

The simulated studies presented in the paper need to be validated in real experimental conditions and this is part of a future work. The SNR advantage obtained for the proposed signal design could be used to enhance the signal analysis and open more advanced analysis features. Bottom characterization in a moving array can be better utilized if single sensor SNR is reasonably good. Each sensor output can be individually used without the requirement of beam forming to enhance SNR. Even other signal design techniques can be attempted if reasonable results are observed during real experimental studies

REFERENCES

[1] P. Qarabaqi and M. Stojanovic, "Statistical characterization and computationally efficient modeling of a class of underwater acoustic

communication channels," *IEEE J. Ocean. Eng.*, vol. 38, no. 4, Oct. 2013, DOI: 10.1109/JOE.2013.2278787.

[2] Urick, R.J. (1954). The backscattering of sound from a harbor bottom. *J. Acoust. Soc. Am.* 26. 231.

[3] Stanton, T.K.: Sound scattering by marine objects. (1994). Lecture Notes. Meeting of Marine Acoustic Society of Japan. 21(4).

[4] Henry M. Manik, Underwater Acoustic Detection and Signal Processing Near the Seabed, Department of Marine Science and Technology Faculty of Fisheries. Available at <http://cdn.intechopen.com/pdfs-wm/18879.pdf>.

[5] Franck Florin, Franck Fohanno, Isabelle Quidu, Jean-Philippe Malkasse. Synthetic Aperture and 3D Imaging for Mine Hunting Sonar. Undersea Defence Technology (UDT) Europe 2004, Jun 2004, Nice, France.

[6] Matthew, W., Franz, H., John, L.: SLAM for Ship Hull Inspection using Exactly Sparse Extended Information Filters. In: 2008 IEEE International Conference on Robotics and Automation, Pasadena, CA, USA, pp. 1463–1470 (2008).

[7] Negahdaripour, S., Sekkati, H., Pirsiavash, H.: Opti-Acoustic Stereo Imaging: On System Calibration and 3-D Target Reconstruction. *IEEE Transactions on Image Processing* 18(6), 1203–1214 (2009).

[8] Marani, G., Choi, S.: Underwater Target Localization. *IEEE Robotics & Automation Magazine* 17(1), 64–70 (2010).

[9] Chen, J., Gong, Z., Li, H., Xie, S.: A Detection Method Based on Sonar Image for Underwater Pipeline Tracker. In: 2011 Second International Conference on Mechanic Automation and Control Engineering (MACE), Hohhot, China, pp. 3766–3769 (2011).

[10] Hao He, Waveform Design for Active Sensing Systems – A Computational Approach, Dissertation presented to the Graduate School of the University of Florida in partial fulfillment of the requirements for the degree of Doctor Of Philosophy, University of Florida, Aug 2011.

[11] Paul C Etter, Underwater Acoustic Modeling and Simulation, Fourth Edition, CRC Press, Taylor and Francis Group, Boca Raton, London, New York, 2013.

[12] N. Chotiros and V. Pallayil, "Seabed characterization using acoustic communication signals on an autonomous underwater vehicle with a thin-line towed array," *IEEE Journal of Oceanic Engineering*, vol. 38, no. 3, pp. 410–418, 2013.

[13] G. L. Turin, "An introduction to matched filters," *IRE Transactions on Information Theory*, vol. 6, pp. 311–329, June 1960.

[14] C. W. Holland, P. L. Nielsen, J. Dettmer, and S. E. Dosso, "Resolving meso-scale seabed variability using reflection measurements from an autonomous underwater vehicle," *J. Acoust. Soc. Am.* 131, 1066–1078 (2012).

[15] P. Stoica, J. Li, and M. Xue, "Transmit codes and receive filters for radar," *IEEE Signal Processing Magazine*, vol. 25, no. 6, pp. 94–109, November 2008.

[16] J. Capon, "High resolution frequency-wavenumber spectrum analysis," *Proceedings of the IEEE*, vol. 57, pp. 1408–1418, August 1969.

[17] P. Stoica, H. Li, and J. Li, "A new derivation of the APES filter," *IEEE Signal Processing Letter*, vol. 6, no. 8, pp. 205–206, August 1999.

[18] T. Yardibi, J. Li, P. Stoica, M. Xue, and A. B. Baggeroer, "Source localization and Sensing: A non parametric iterative adaptive approach based on weighted least squares," *IEEE Transactions on Aerospace and Electronic Systems*, vol. 46, no. 1, pp. 425 – 443, Jan. 2010.

[19] Fowle E N, Design of FM pulse compression signals, *IEEE Transactions on Information Theory*, Vol. 10, No. 1, 61-67, 1964.

[20] J.A. Johnston, A.C. Fairhead, "Waveform design and Doppler sensitivity analysis for nonlinear FM chirp pulses", *IEE Proc. F.*, 2, 163 – 175.

[21] Y K Chan, M Y Chua and V C Koo, "Sidelobes Reduction using simple two and tri-stages Non linear frequency modulation (NLFM)", *Progress in Electromagnetics Research*, PIER 98, 2009.

[22] David J Battle, Peter Gerstoft, William A Kuperman, William S Hodgkiss and Martin Siderius, "Geoacoustic Inversion of Tow-Ship Noise via Near Field Matched Field Processing", *IEEE Journal of Oceanic Engineering*, Vol 28, No. 3, Jul 2003.

- [23] P. H. Rogers, Onboard prediction of propagation loss in shallow water, 16 Sep 1981: Applied Ocean, Acoustics Branch, Acoustics Division, Naval Research Lab, Washington, DC. Available at <http://www.dtic.mil/dtic/tr/fulltext/u2/a104738.pdf>.
- [24] Harris, E. J., "On the use of windows for harmonic analysis with the discrete fourier transform", Proc. IEEE, Vol. 66, No. 1, 51-83, 1978.
- [25] Giovanni Toso, Paolo Casari, Michele Zorzi, "The Effect of Different Attenuation Models on the Performance of Routing in Shallow-Water Networks". Available at [http://telecom.dei.unipd.it/media/download/411/..](http://telecom.dei.unipd.it/media/download/411/)